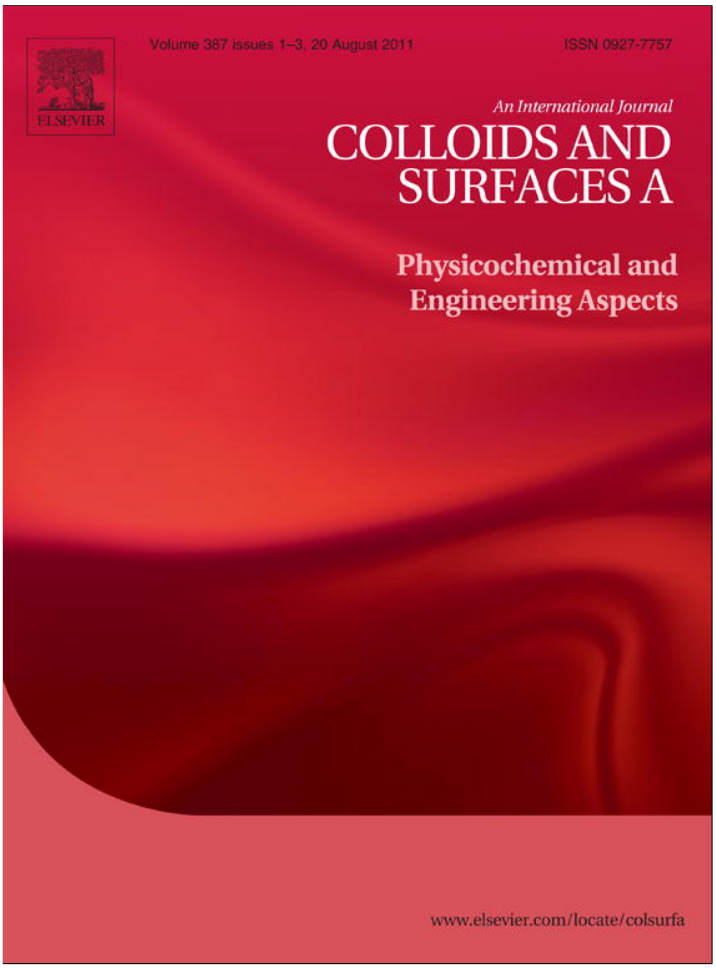

Colloids and Surfaces A: Physicochem. Eng. Aspects 387 (2011) 50–56

Contents lists available at ScienceDirect

Colloids and Surfaces A: Physicochemical and Engineering Aspects

journal homepage: www.elsevier.com/locate/colsurfa

# Adsorption comparison at the α-alumina/water interface: 3,4-Dihydroxybenzoic acid vs. catechol

Jayanta M. Borah, Jyotirmoy Sarma, Sekh Mahiuddin*

*Materials Science Division, North-East Institute of Science and Technology, CSIR, Jorhat 785006, Assam, India*

ARTICLE INFO

*Article history:*
Received 15 March 2011
Received in revised form 9 July 2011
Accepted 14 July 2011
Available online 23 July 2011

*Keywords:*
Adsorption
α-Alumina
Catechol
3,4-Dihydroxybenzoic acid
DRIFT spectra
Kinetics

ABSTRACT

Adsorption kinetics and isotherms and the surface complexation of 3,4-dihydroxybenzoic acid (3,4-DHBA) and catechol at the α-alumina/electrolyte interface were investigated. The state of equilibrium for adsorption of 3,4-DHBA onto α-alumina surface at pH 5 was attained at 120 min, whereas it was 90 min for catechol, but at pH 10 the state of equilibrium for the both the systems was same (~60 min). The pseudo-second-order kinetic equation of nonlinear form (Eq. (3)) fits the experimental kinetic data significantly better than the linear form (Eq. (2)) in the entire time duration. The adsorption density of 3,4-DHBA onto the α-alumina surfaces at pH 10 and at similar experimental conditions is equivalent to catechol. DRIFT spectra indicate that 3,4-DHBA forms both outer- and inner-sphere complexes and catechol forms bidentate mononuclear complex with the α-alumina surface.



## 1. Introduction

Polyhydroxybenzoic acids are important components in the aquatic eco-system [1,2] and are responsible for a variety of processes that take place in the biosphere including accessibility of micronutrients for plants and several environmentally important geochemical processes such as mineral dissolution, metal-ion sequestration, redox reaction, pH buffering and stability of mineral colloids [3–6]. Dihydroxybenzoic acids (DHBAs) are produced by degradation of vegetative matters [7,8], they are used as important intermediates of many industrial synthetic processes [9,10] and are equally undesirable as pollutants in the biosphere, e.g., 2,3-DHBA, 3,4-DHBA, and 2,5-DHBA are major organic pollutants in the agro-industrial waste water [11,12]. On the other hand, phenolic compounds such as catechol and its derivatives are distributed in aquatic environment contributed by industrial effluent from textile, petrochemical refinery, pharmaceutical and industries [11].

The adsorption of phenolic acid and its analogues onto metal-oxide and oxy(hydroxide) minerals through the polar –COOH and/or phenolic –OH functional groups has been reported in the literature [13–18]. Parenthetically we remark that the adsorption and surface complexation of DHBAs onto metal oxide surfaces primarily depend on the pH of the suspension [19,20] and the position and numbers of ionizable polar functional groups. The position of phenolic –OH group either in *ortho* or *para* or both positions in DHBA is likely to increase the electron density within the benzene ring and $–COO^-$ due to strong electron resonating and the inductive effects resulting in significant increase in adsorption density of the DHBA onto the mineral surface [13,18,21]. Further, at alkaline pH the phenolic –OH groups in DHBA, one of them either in *ortho* or *para* position, are also participate in adsorption process. The adsorption of DHBA onto mineral oxide at acidic pH is primarily through the –COOH and at alkaline pH through the phenolic –OH group(s) [13].

Results showed that the position of the –COOH groups in benzenetricarboxylic acids is one of governing factors for different adsorption densities at a fixed pH onto an adsorbent [14,18,21]. Note that no correlation could be established between the adsorption density and the $pK_a$ for benzenetricarboxylic acids. On the other hand, the DHBAs exhibit quite interesting variation of adsorption density and the summarized results are: (i) the phenolic –OH group(s) increases the interaction of $–COO^-$ causing higher adsorption density, (ii) phenolic –OH group at *ortho* position is important at acidic pH while for alkaline pH the adjacent phenolic –OH groups primarily govern the adsorption density [13]. Further, Guan et al. [13] showed that the magnitude of the adsorption density of DHBAs has significant correlation with their first $pK_a$, which was not followed for the benzenetricarboxylic acids. This relationship was observed at pH 6. Now question arises, is the correlation (adsorption density vs. $pK_a$) followed for DHBAs at alkaline pH, since the phenolic –OH groups are deprotonated and 3,4-DHBA is likely to

* Corresponding author. Tel.: +91 0376 2370081; fax: +91 0376 2370011.
*E-mail addresses:* mahirrljt@yahoo.com, mahiuddins@rrljorhat.res.in (S. Mahiuddin).

0927-7757/$ – see front matter © 2011 Elsevier B.V. All rights reserved.
doi:10.1016/j.colsurfa.2011.07.024

behave like catechol [18]. Further, no detailed adsorption isotherms for 3,4-DHBA onto any adsorbent are reported in a wide pH range. Parenthetically we note that the adsorption profile of 3,4-DHBA would be different at acidic and alkaline pH.

In this paper, a comparative adsorption behaviour of 3,4-DHBA and catechol onto α-alumina surface are presented. The reason for incorporation of catechol in the present study is to examine the increase in adsorption density of 3,4-DHBA at alkaline pH and to compare their adsorption behaviour. We discussed adsorption kinetics at a fixed pH, the adsorption isotherms at different pH and the surface complexations of 3,4-DHBA and catechol onto α-alumina surfaces.

## 2. Materials and methods

### 2.1. Materials

Alumina (>99%, Aldrich, Germany) was washed twice with double distilled water, dried and desiccated over calcium chloride (>95%, s.d. fine-chem, India). The surface area of the α-alumina is 7.29 $m^2\ g^{-1}$, determined by the BET method. 3,4-DHBA (>97%, Lancaster, UK) and catechol (>99%, Himedia, India), sodium hydroxide (>99%, s.d. fine-chem, India), hydrochloric acid (A.R. grade, NICE chemicals, India), and sodium hydroxide (A.R. grade, Merck, India) were used without further purification.

### 2.2. Adsorption kinetics

Adsorption kinetics of 3,4-DHBA and catechol onto α-alumina (0.5 g) in a 15 mL suspension were performed by batch process at pH 5 and four temperatures viz., 288.15, 298.15, 303.15 and 313.15 K. The initial concentrations of 3,4-DHBA and catechol and other experimental conditions are noted in the respective figure captions. A series of the suspensions containing α-alumina in the presence of 0.05 mM NaCl(aq) were thoroughly mixed by using a vortex mixer and equilibrated for one hour in a shaking water bath (LT-10F, Titec, Japan) maintained at a desired temperature with constant shaking and then desired amount of an adsorbate was added. The suspension was filtered through a membrane of 0.2 μm pore size at different intervals of time. The residual concentration of 3,4-DHBA and catechol was estimated at the corresponding absorption maxima, $\lambda_{max}$, 249 and 192.2 nm, respectively with an UV–visible spectrophotometer, Specord 200 (Analytic Jena, Germany). The adsorption density, $\Gamma$, of an adsorbate was estimated by following mass balance equation:

$$\Gamma = \frac{(C_0 - C_e)V}{ma} \quad (1)$$

where $C_0$ and $C_e$ are the initial and residual concentration (mM) of an adsorbate in the suspension, $V$ is the total volume of the suspension taken, $m$ and $a$ are the mass and surface area of the adsorbent, respectively.

### 2.3. Adsorption isotherms

A suspension of 15 mL containing 0.5 g α-alumina and 0.05 mM NaCl in a screw-capped glass tube was mixed thoroughly with the help of a vortex mixer. The desired pH of the suspension was adjusted by adding either dilute NaOH or HCl solution using a pH meter (Systronics, India) and equilibrated for 1 h at 298.15 K in a shaking water bath. The required amount of adsorbate (3,4-DHBA or catechol) solution was added and the pH of the suspension was readjusted, if necessary. After the reaction period elapsed (adsorption equilibration time = 2 h) the suspension was filtered through a membrane of 0.2 μm pore size and the residual concentration was estimated as noted in the previous section.

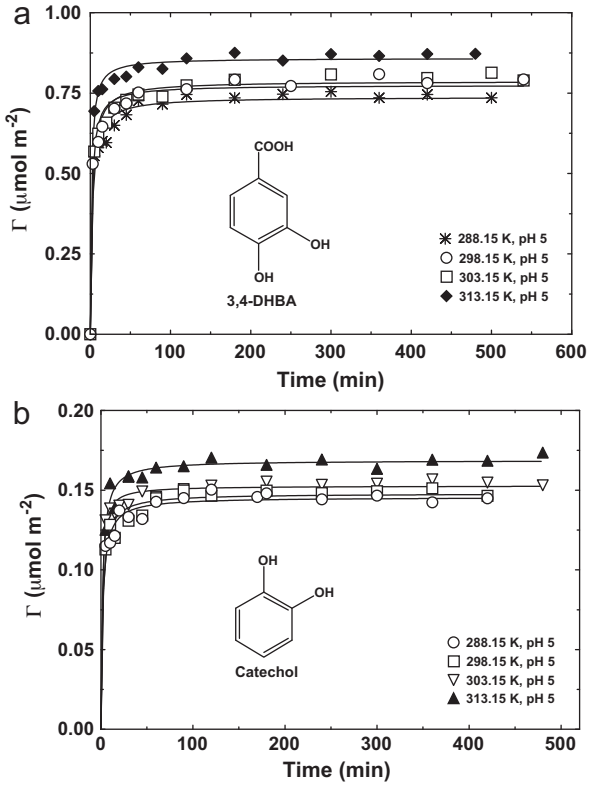


**Fig. 1.** Effect of temperature on the adsorption kinetics of (a) 3,4-DHBA onto α-alumina surface at a fixed initial concentration: $C_0$ = 0.25 mM, α-alumina = 0.5 g, NaCl(aq) = 0.05 mM, $V$ = 15 mL, and pH 5 and 10 and (b) catechol onto α-alumina surface at a fixed initial concentration of catechol: $C_0$ = 0.05 mM, α-alumina = 0.5 g, NaCl(aq) = 0.05 mM, $V$ = 15 mL, and pH 5. Symbols are experimental and solid lines are the theoretical value (Eq. (3)). The data points represent triplicate adsorption kinetics experiments. For fitting of the experimental data to Eq. (3) unit of $q_t$ was taken into account. Molecular structures of 3,4-DHBA and catechol are shown in the respective plots.

### 2.4. Diffuse reflectance infrared Fourier transform spectra (DRIFT)

For DRIFT spectra, 0.5 g α-alumina was equilibrated with 1 mM 3,4-DHBA and catechol, respectively, in the presence of 0.05 mM NaCl(aq) for 2 h at different pH 5–10 and 298.15 K. The suspension were filtered and washed once with double distilled water. The adsorbent was dried in a vacuum desiccator over fused calcium chloride. The DRIFT spectra were recorded with a FTIR-Spectrum-100 (PerkinElmer, USA) with a resolution of 4 $cm^{-1}$.

## 3. Results and discussion

### 3.1. Adsorption kinetics

The adsorption densities, $\Gamma$ (μmol $m^{-2}$), of 3,4-DHBA and catechol onto α-alumina surfaces at pH 5 as a function of time in the presence of 0.05 mM NaCl(aq) are shown in Fig. 1. The time taken to attain the state of equilibrium is 120 min for 3,4-DHBA/α-alumina and 90 min for catechol/α-alumina systems within the temperature range of the study. In comparison to 3,4-DHBA, catechol has lower adsorption equilibration time and numerically ~1.3 times less than 3,4-DHBA.

In Section 1 we mentioned that the adsorption behaviour of 3,4-DHBA would be similar to catechol at alkaline pH. To examine this behaviour adsorption kinetics were carried out at pH 10 keeping the initial concentrations of 3,4-DHBA and catechol (a) different as in Fig. 1 and (b) equal and the typical plots are also shown in Fig. 2. The results showed that the state of equilibrium at pH 10, under

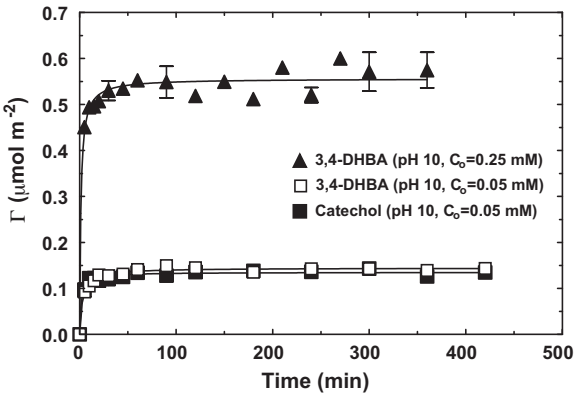


**Fig. 2.** Adsorption kinetics of 3,4-DHBA and catechol onto α-alumina surface at pH 10 keeping (a) $C_0$ different as in Fig. 1 and (b) $C_0$ = 0.05 mM. The data points represent triplicate adsorption kinetics experiments. For fitting of the experimental data to Eq. (3) unit of $q_t$ was taken into account.

two different conditions, for both the systems is reached within 60 min. The kinetics results, under similar experimental conditions, indicate that the adsorption density of 3,4-DHBA is numerically equal to that of catechol (Fig. 2). Note that the equilibration time and the adsorption density at surface saturation also depend on the pH of the suspension and the initial concentration of an adsorbate.

With the pseudo-first-order kinetic equation a large deviation (up to ~90%) between the experimental and calculated adsorption density at equilibrium was observed and the reasons of such deviation are reported by many authors [22–28]. Therefore, we restricted to pseudo-second-order kinetics and the experimental kinetics data of both the systems were fitted to pseudo-second-order kinetic equations of both linear and non-linear forms:

$$\frac{t}{q_t} = \frac{1}{k_l q_e^2} + \frac{t}{q_e} \tag{2}$$

$$q_t = \frac{k_{nl} q_e^2 t}{k_{nl} q_e t + 1} \tag{3}$$

where $k_l$ and $k_{nl}$ are the rate constants of pseudo-second-order kinetic equation of linear and non-linear forms and $q_t$ and $q_e$ are the adsorption densities of 3,4-DHBA onto α-alumina at time $t$ and at equilibrium, respectively. The estimated values of $q_e$, $k_l$ and $k_{nl}$ of both the systems are listed in Table 1. The magnitude of deviation is significantly reduced for estimation of $q_e$ using pseudo-second-order kinetic equations of linear (~12%) and non-linear (~3%) forms. The pseudo-second-order kinetic equation of non-linear form is found to be better model for estimation of kinetic parameters for both the systems, as the associated statistical errors are minimized [22,24,25]. Further, the activation energy, $E_a$, is calculated by using Arrhenius equation,

$$\ln k_{nl} = \ln A - \frac{E_a}{RT} \tag{4}$$

where $A$ is the Arrhenius pre-exponential factor, $R$ is the universal gas constant and $T$ is the temperature in Kelvin. The activation energy for the adsorption of catechol onto α-alumina surface at pH 5 is found to be lower (2.13 kJ/mol) than that of 3,4-DHBA onto α-alumina (10.5 kJ/mol) surfaces. It implies that at pH 5 adsorption of catechol onto α-alumina surfaces is faster (~4.9 times) than 3,4-DHBA, which leads to lower adsorption equilibration time.

### 3.2. Adsorption isotherms

The variations of adsorption densities of 3,4-DHBA and catechol at the α-alumina/electrolyte interface with different initial concentrations of the corresponding adsorbate in the presence of 0.05 mM

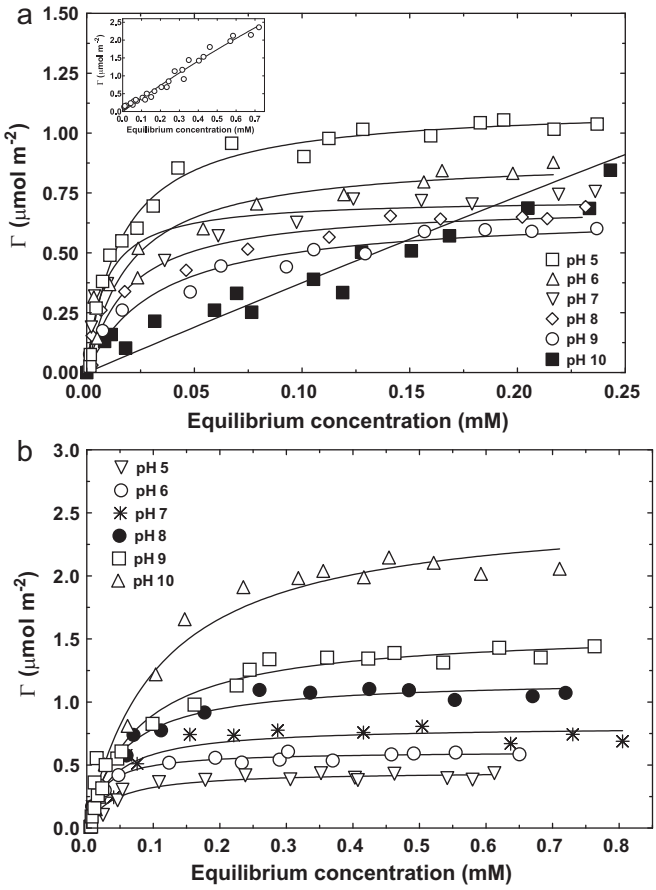


**Fig. 3.** Adsorption isotherms of (a) 3,4-DHBA onto α-alumina surface at different pH, fixed concentration of NaCl(aq) = 0.05 mM, α-alumina = 0.5 g, $V$ = 15 mL, and 298.15 K. Inset: adsorption isotherm of 3,4-DHBA onto α-alumina surface at pH 10 and (b) catechol onto α-alumina surface at different pH, fixed concentration of NaCl(aq) = 0.05 mM, α-alumina = 0.5 g, $V$ = 15 mL and 298.15 K. Symbols are experimental and solid lines are the theoretical value (Eq. (4)) and the SI unit of $\Gamma$ and $C_e$ was taken into account. The data points represent triplicate adsorption experiments.

NaCl(aq) as a function of pH at 298.15 K are shown in Fig. 3. The experimental data were fitted to Langmuir adsorption isotherm equations of the following form:

$$\Gamma = \frac{\Gamma_{\max} C_e}{K + C_e} \tag{5}$$

where $K = 1/K_s$, $K_s$ ($dm^3\ mmol^{-1}$) is the adsorption co-efficient, $\Gamma$ and $\Gamma_{max}$ are the adsorption densities of adsorbate in $\mu mol\ m^{-2}$ at equilibrium and after saturation of α-alumina surface and $C_e$ ($mmol\ dm^{-3}$) is the concentration of adsorbate at equilibrium in the supernatant liquid, respectively. The estimated values of the parameters of Eq. (5) for both the systems are listed in Table 2. However the adsorption densities at pH 5 and 10 for both the systems were fitted to the Freundlich adsorption isotherm equation,

$$\Gamma = K_f C_e^n \tag{6}$$

where $K_f$ ($(\mu mol\ m^{-2})/(mmol^{-n}\ dm^{-(3+n)})$) and $n$ are the Freundlich co-efficient, representing the adsorption capacity and the adsorption intensity, respectively. Typical comparison plots of Langmuir and Freundlich equations for both the systems at pH 5 and 10 are shown in Figs. 1S and 2S (Supporting Materials) and the best fitted values are given in Table 1S (Supporting Materials). The standard deviations (Table 1S) and the curve fitting (Figs. 1S and 2S) indicate that the Langmuir is the better model than the Freundlich model for the present systems except at pH 10 where both the models are equally applicable (Table 1S). The adsorption isotherm with a

**Table 1**
Values of the rate constants and equilibrium concentration for adsorption of 3,4-DHBA/α-alumina and catechol/α-alumina systems.

| Equation | Parameters | 288.15 K | 298.15 K | 303.15 K | 313.15 K |
|---|---|---|---|---|---|
| **3,4-DHBA/α-alumina system at pH 5** | | | | | |
| Eq. (2) | $k_1$ (μmol$^{-1}$ m$^2$ min$^{-1}$) | 0.331 | 0.469 | 0.426 | 0.567 |
| | $q_e$ (μmol m$^{-2}$) | 0.761 | 0.778 | 0.782 | 0.860 |
| | S.D. | 0.049 | 0.090 | 0.089 | 0.123 |
| Eq. (3) | $k_{nl}$ (μmol$^{-1}$ m$^2$ min$^{-1}$) | 0.550 | 0.680 | 0.523 | 0.839 |
| | $q_e$ (μmol m$^{-2}$) | 0.738 | 0.775 | 0.787 | 0.859 |
| | S.D. | 0.028 | 0.033 | 0.025 | 0.019 |
| Experimental | $q_e$ (μmol m$^{-2}$) | 0.732 | 0.753 | 0.777 | 0.851 |
| **Catechol/α-alumina system at pH 5** | | | | | |
| Eq. (2) | $k_1$ (μmol$^{-1}$ m$^2$ min$^{-1}$) | 2.283 | 1.905 | 4.623 | 2.985 |
| | $q_e$ (μmol m$^{-2}$) | 0.148 | 0.153 | 0.152 | 0.168 |
| | S.D. | 0.010 | 0.024 | 0.006 | 0.007 |
| Eq. (3) | $k_{nl}$ (μmol$^{-1}$ m$^2$ min$^{-1}$) | 3.537 | 3.569 | 6.042 | 3.418 |
| | $q_e$ (μmol m$^{-2}$) | 0.146 | 0.148 | 0.153 | 0.169 |
| | S.D. | 0.006 | 0.006 | 0.004 | 0.005 |
| Experimental | $q_e$ (μmol m$^{-2}$) | 0.144 | 0.149 | 0.154 | 0.168 |

**Table 2**
Values of parameter of Langmuir adsorption as a function of pH for adsorption of 3,4-DHBA/α-alumina and catechol/α-alumina systems at 298.15 K.

| pH | 3,4-DHBA/α-alumina | | | Catechol/α-alumina | | |
|---|---|---|---|---|---|---|
| | $\Gamma_{max}$ (μmol m$^{-2}$) | $K_s$ (dm$^3$ mmol$^{-1}$) | S.D. | $\Gamma_{max}$ (μmol m$^{-2}$) | $K_s$ (dm$^3$ mmol$^{-1}$) | S.D. |
| 5 | 1.115 ± 0.020 | 62.42 ± 5.14 | 0.040 | 0.452 ± 0.017 | 24.75 ± 5.28 | 0.034 |
| 6 | 0.901 ± 0.050 | 50.97 ± 12.14 | 0.076 | 0.609 ± 0.012 | 43.20 ± 4.53 | 0.027 |
| 7 | 0.726 ± 0.032 | 121.8 ± 33.55 | 0.067 | 0.809 ± 0.046 | 26.01 ± 8.01 | 0.085 |
| 8 | 0.702 ± 0.030 | 52.46 ± 11.51 | 0.048 | 1.186 ± 0.032 | 19.69 ± 2.60 | 0.055 |
| 9 | 0.668 ± 0.037 | 30.84 ± 6.99 | 0.041 | 1.572 ± 0.055 | 13.32 ± 1.80 | 0.095 |
| 10 | 18.71 ± 10.78 | 0.204 ± 0.129 | 0.112 | 2.546 ± 0.100 | 9.390 ± 1.327 | 0.118 |

plateau, i.e., surface saturation or in other words, for perfect monolayer adsorption behaviour, the Langmuir equation is better than the Freundlich equation.

The adsorption densities of 3,4-DHBA onto α-alumina (Fig. 3a) increase with the increase in equilibrium concentration of 3,4-DHBA and a plateau is reached upon surface saturation that provides $\Gamma_{max}$. On the other hand, adsorption density upon surface saturation, $\Gamma_{max}$, decreases with the increase in pH of the medium in the pH range 5–9 but at pH 10 the adsorption behaviour is different wherein the adsorption density gradually increases with the increase in 3,4-DHBA concentration and no plateau, a signature of surface saturation, is obtained. The increase in adsorption density of 3,4-DHBA onto alumina at pH 10, to our best knowledge, is not reported in the literature. Nevertheless Evanko and Dzombak [18] reported the adsorption isotherms of all DHBAs and catechol up to pH ≤ 9, therefore, the adsorption behaviour of 3,4-DHBA and catechol onto alumina needs attention for comparison at pH ≥ 9. In contrast, the adsorption densities of DHBAs where two –OH groups are not adjacent, e.g., 2,4- and 3,5-DHBA, do not increase at pH 10 [21]. Therefore, the increase in adsorption density of 3,4-DHBA at pH 10 indicates that the two phenolic –OH groups are ionized (the first –OH group is fully and second –OH group partially, p$K_{a2}$ = 9.08 and p$K_{a3}$ = 12.58) [13,18] and their participation in the surface complexation. The adsorption behaviour of 3,4-DHBA at a fixed initial concentration and pH 10 is in tune with catechol (Fig. 2) and further explained by taking adsorption isotherms of catechol as reference.

For explaining the higher adsorption density of 3,4-DHBA (p$K_{a1}$ = 4.46, p$K_{a2}$ = 9.08 and p$K_{a3}$ = 12.58) at pH 10 we present the UV spectra of 3,4-DHBA along with the catechol (p$K_{a1}$ = 9.34 and p$K_{a2}$ = 13.24) at a common concentration (0.1 mM) and different solution pH. The spectra of 3,4-DHBA are insensitive up to pH 8.5, while for catechol the spectra are insensitive up to pH 8 (Fig. 4). Comparing the spectral pattern of two phenolic compounds and incipient spectral changes at the respective higher pH it is evident that the onset of deprotonation of 3,4-DHBA begins at pH > 9 with shifting of $\lambda_{max}$ to higher wavelength [29,30] and therefore, the

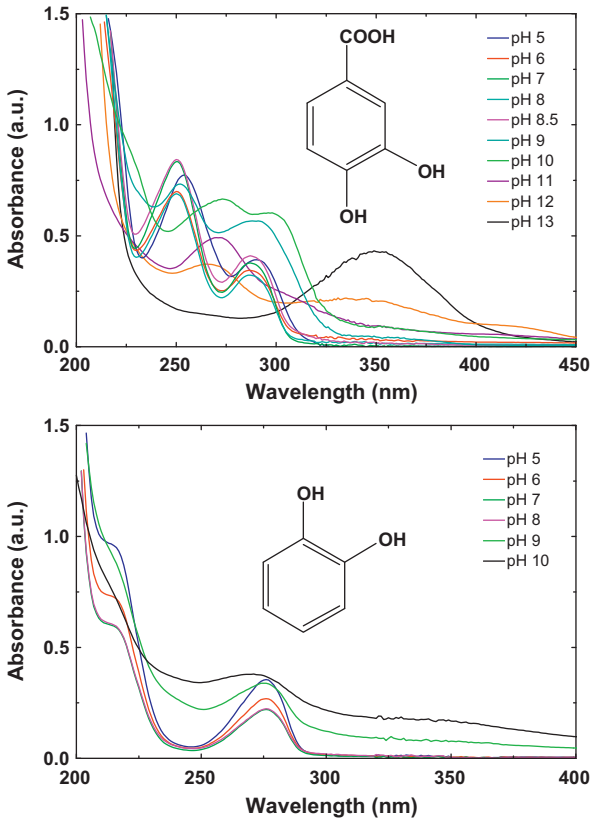


**Fig. 4.** UV spectra of 0.1 mM 3,4-DHBA (upper panel) and catechol (lower panel) as a function of pH. The shifting and shape of the spectrum at pH > 9 demonstrate the onset of deprotonation in both phenolic compounds. Molecular structures of 3,4-DHBA and catechol are shown in the respective plots.

participation of 3,4-DHBA in the adsorption process through –OH group at pH 10 is evident.

From the adsorption isotherms of catechol/α-alumina at pH 5–10 at 298 K (Fig. 3b), it is apparent that adsorption densities increase with the increase in suspension pH. The adsorption density is maximum at pH 10 since two adjacent –OH groups are deprotonated causing favorable for adsorption onto α-alumina with the increase in adsorption density [13,18]. The adsorption of catechol onto α-alumina surfaces is Langmurian in nature [31] and the estimated values of the parameters of Eq. (5) are given in Table 2.

Now, we compare the adsorption density of 3,4-DHBA and catechol onto α-alumina at a common pH. Taking $\Gamma_{max}$ as reference (Table 2) note that the adsorption density of 3,4-DHBA in comparison to catechol is ~2.5 times higher at pH 5, which decreases with the increase in suspension pH up to 9 and surprisingly a sharp increase in adsorption density (~7.3 times) is observed at pH 10. The results indicate that the higher adsorption density of 3,4-DHBA at both pH (5 and 10) is linked with the position of the –OH group. The literature showed that the interaction energy of 3,4-DHBA is higher than catechol [32]. The electron of –OH group at *para* position increases the electron density of the benzene ring and may be in –COOH carboxyl group because of electron resonating and donating effects resulting in higher interaction energy of 3,4-DHBA.

### 3.3. DRIFT spectroscopy

#### 3.3.1. 3,4-DHBA/α-alumina

The DRIFT spectra of α-alumina treated with 1 mM 3,4-DHBA at different pH in the presence of 0.05 mM NaCl(aq) are shown in Fig. 5a and the characteristic peaks are listed along with 3,4-DHBA and its salt in Table 3 and are in good agreement with the reported data [13]. The C–OH stretch and bending of 3,4-DHBA appear at 1246 and 1287 $cm^{-1}$, respectively. The peaks at 1418 and 1526 $cm^{-1}$ correspond to $\nu_{C-C}$ ring stretch, which interfere with the peak positions of $\nu_s(-COO^-)$ and $\nu_{as}(-COO^-)$ as they appear in these region and subsequent interpretation. To ascertain the peak position of $\nu_s(-COO^-)$ and $\nu_{as}(-COO^-)$ the DRIFT spectra of Na-salt of 3,4-DHBA are also included in Fig. 5a. The peak at 1600 $cm^{-1}$ represents $\nu_{C-C}$ and $\nu_{C-O}$ [13,33,34] and 1671 $cm^{-1}$ is due to the >C=O stretch [35]. On comparing the spectra of 3,4-DHBA and its salt, we ascertain that the peaks at 1546 and 1397 $cm^{-1}$ correspond to $\nu_{as}(-COO^-)$ and $\nu_s(-COO^-)$, respectively and are in good agreements with the literature [13]. Worth noting that the peak intensities associated with $\nu_{C-C}$ and $\nu_{C=O}$ for sodium salt of 3,4-DHBA significantly decrease with the shifting of position that accounts for the ionization of –COOH group and appearance of $\nu_{as}(-COO^-)$ and $\nu_s(-COO^-)$ at 1546 and 1397 $cm^{-1}$, respectively. After adsorption of 3,4-DHBA onto α-alumina surfaces the peak corresponds to $\nu_s(-COO^-)$ red shifted by ~25 $cm^{-1}$ and centered at 1372 ± 2 $cm^{-1}$ in all pH ranges. The peak corresponds to $\nu_{as}(-COO^-)$ is also red shifted by ~40 $cm^{-1}$ but the intensity of $\nu_s(-COO^-)$ and $\nu_{as}(-COO^-)$ decreases as the pH of the suspension increases. The intensity of $\nu_{as}(-COO^-)$ becomes very weak at pH 9 and 10. The band in the range 1629–1635 $cm^{-1}$ could not be distinguished amongst $\nu_{as}(\alpha\text{-}COO^-)$, $\nu_{as}(\gamma\text{-}C{=}O)$ and water. However, we note that the peak in the 1629–1635 $cm^{-1}$ range after adsorption (Fig. 6a) represents C–C stretching vibrations (~1600 $cm^{-1}$ for 3,4-DHBA [36]). The peaks at 1246 and 1287 $cm^{-1}$ correspond to phenolic –OH stretching and bending of 3,4-DHBA. The corresponding stretching and bending modes of C–O(H) in salt become more prominent with doublet in 1200–1246 $cm^{-1}$ and blue shifted by 10 $cm^{-1}$ with a shoulder. The peaks due to C–O(H) phenolic bending and stretching of 3,4-DHBA upon adsorption are not distinguishable and a single and strong peak appears at 1277 ± 1 $cm^{-1}$ [36] and the intensity of the peak decreases with the increase in pH of the suspension. Therefore, the peak at 1277 ± 1 $cm^{-1}$ with decrease

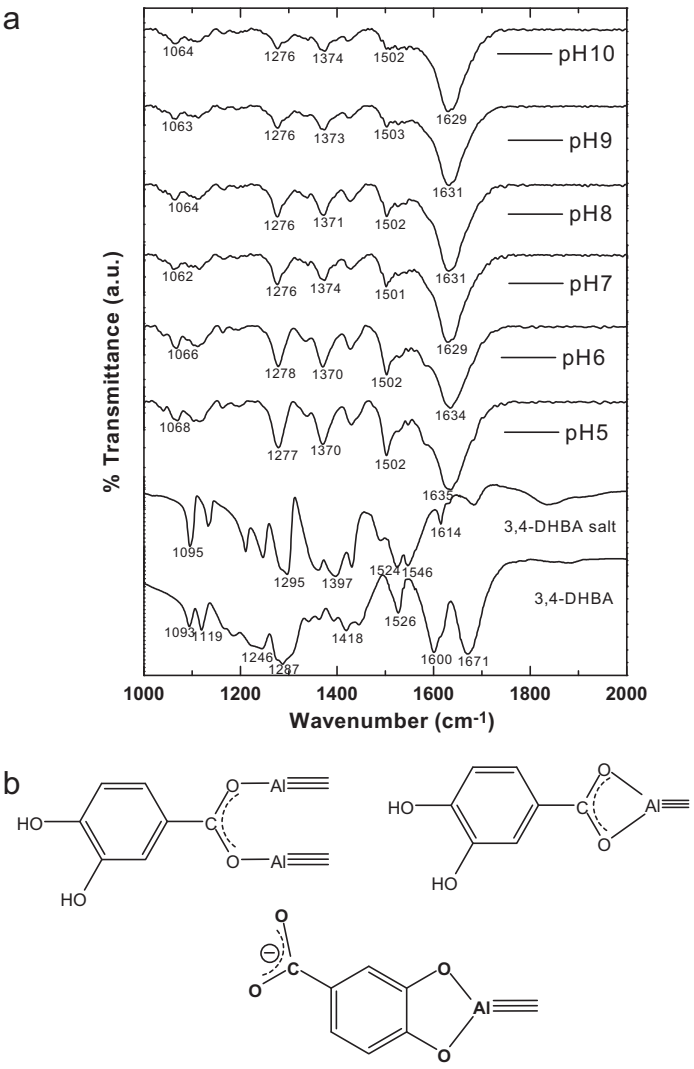


**Fig. 5.** (a) DRIFT spectra of 3,4-DHBA, sodium salt of 3,4-DHBA and 3,4-DHBA after adsorption onto α-alumina surface at pH 5–10 in presence of 0.05 mM NaCl(aq), $C_0$ = 1 mM and at 298.15 K and (b) schematic representation of both outer- and inner-sphere surface complexation of 3,4-DHBA onto α-alumina.

in intensity indicates the participation of phenolic –OH group in the surface complexation of 3,4-DHBA onto α-alumina [13,36]. The band separation between $\nu_s(-COO^-)$ and $\nu_{as}(-COO^-)$ is employed to distinguish the co-ordination modes of an adsorbate with metal oxides surfaces [37,38]. Surface complexation of a series of DHBA onto aluminium hydroxide surface at pH 5 has been reported and they form inner-sphere complexes with aluminium hydroxide surface [13].

The peak at 1119 $cm^{-1}$ corresponds to C–H bending vibrations [34] becomes weak and broad after adsorption. The peak at 1671 $cm^{-1}$ for C=O(–COOH) stretching of 3,4-DHBA [35] becomes weak of the salt indicates that the –COOH group of the salt prepared at pH 6 is not fully ionized and disappears after adsorption. From adsorption isotherms (Fig. 2a) and spectroscopic data reveal that the phenolic group is important in alkaline pH and carboxylic group in acidic pH for adsorption and surface complexation of 3,4-DHBA onto alumina surface. For inner-sphere complex formation on the mineral oxide surface the shifting of $\nu_{as}(-COO^-)$ and $\nu_s(-COO^-)$ should be of higher magnitude ($\geq$40 $cm^{-1}$) The magnitude of shifting $\nu_{as}(-COO^-)$ towards lower frequency after adsorption indicates that 3,4-DHBA forms both outer- and inner-sphere complexes with

**Table 3**
Characteristic peak frequencies of 3,4-DHBA and catechol upon adsorption onto α-alumina surface.

| Vibration | $\nu$ ($cm^{-1}$) | | | | | | | |
|---|---|---|---|---|---|---|---|---|
| | 3,4-DHBA | 3,4-DHBA salt | pH 5 | pH 6 | pH 7 | pH 8 | pH 9 | pH 10 |
| **3,4-DHBA/α-alumina system** | | | | | | | | |
| $\nu_s$ ($-COO^-$) | | 1397 | 1370 | 1370 | 1374 | 1371 | 1373 | 1374 |
| $\nu_{as}$ ($-COO^-$) | | 1546 | 1502 | 1502 | 1501 | 1502 | 1503 | 1502 |
| C–O(H) phenolic bending | 1287 | 1295 | 1277 | 1278 | 1276 | 1276 | 1276 | 1276 |
| $\nu_{C-C}$ (ring stretch) | 1418 | 1430 | 1430 | 1428 | 1428 | 1427 | 1425 | 1423 |
| | 1526 | | | | | | | |
| $\nu_{C=O}$ | 1671 | 1682 | | | | | | |
| $\nu$(C–H) (in plane bending) | 1119 | 1133 | 1116 | 1111 | 1115 | 1113 | 1112 | 1114 |
| | 1093 | 1095 | 1068 | 1066 | 1062 | 1064 | 1063 | 1064 |
| $\nu_{C-C}$ (ring) | 1600 | 1614 | 1635 | 1634 | 1629 | 1631 | 1631 | 1629 |
| C–O(H) phenolic stretch | 1246 | 1246 | 1277 | 1278 | 1276 | 1276 | 1276 | 1276 |
| | | Catechol | pH 5 | pH 6 | pH 7 | pH 8 | pH 9 | pH 10 |
| **Catechol/α-alumina system** | | | | | | | | |
| $\nu_{C-C}$ (ring stretch) | | 1620 | 1633 | 1628 | 1627 | 1635 | 1632 | 1633 |
| | | 1601 | | | | | | |
| $\nu_{C=C}$ stretching | | 1514 | 1493 | 1493 | 1493 | 1493 | 1493 | 1493 |
| | | 1470 | | | | | | |
| C–O(H) bend coupled to C–O stretch | | 1281 | 1257 | 1256 | 1256 | 1256 | 1256 | 1257 |
| | | 1255 | 1167 | 1167 | 1166 | 1167 | 1167 | 1165 |
| | | 1187 | | | | | | |
| C–O(H) stretch | | 1241 | 1257 | 1256 | 1256 | 1256 | 1256 | 1257 |
| C–C ring stretch coupled to C–O(H) bend | | 1364 | 1331 | 1332 | 1334 | 1331 | 1331 | 1331 |
| $\delta_{C-H}$ (in plane) | | 1096 | 1065 | 1064 | 1065 | 1066 | 1065 | 1065 |
| | | 1040 | 1102 | 1102 | 1101 | 1102 | 1101 | 1100 |

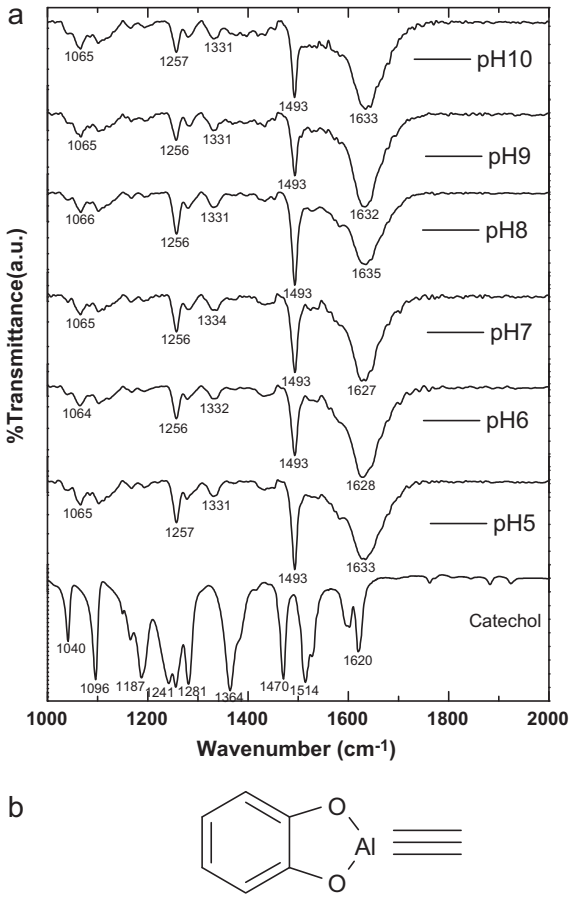


**Fig. 6.** (a) DRIFT spectra of catechol and catechol after adsorption onto α-alumina surface at pH 5–10 in presence of 0.05 mM NaCl(aq), $C_0$ = 1 mM and at 298.15 K and (b) schematic representation of surface complexation of catechol onto α-alumina surfaces.

α-alumina surfaces. The possible surface complexations at acidic and alkaline pH are shown in Fig. 5b.

### 3.3.2. *Catechol/α-alumina system*

The important and characteristic peaks of catechol and catechol after adsorption onto α-alumina surface at different pH are shown in Fig. 6a and Table 3 and the peak frequencies are in good agreement with literature values [13,31,39–42]. Recently Gulley-Stahl et al. [39] reported the surface complexation of catechol with four metal oxides surface using in situ ATR-FTIR technique. They reported that catechol binds with manganese dioxide surface predominantly by outer-sphere complex and iron (III), titanium and chromium (III) oxides and forms inner-sphere complexes. The peak at 1514 $cm^{-1}$ corresponds to $\nu_{C=C}$ aromatic ring stretching for free catechol. This peak red shifted as a sharp peak at 1493 $cm^{-1}$ after adsorption at all pH ranges. The $\nu_{C-O(H)}$ stretching with doublet at ~1241 $cm^{-1}$ shifted to higher frequency and centered at ~1256 $cm^{-1}$ [43]. Similarly, the $\nu_{C-O(H)}$ bending vibration at 1281 $cm^{-1}$ also shifted as a single and strong peak at 1256 $cm^{-1}$. The doublet at around 1620 $cm^{-1}$ corresponds to $\nu_{C-C}$ stretching appears as a relatively broad peak at 1627–1635 $cm^{-1}$ range after adsorption due to absorbed water [31]. The peak at 1364 $cm^{-1}$ is assigned to $\nu_{O-H}$ vibration coupled with aromatic C–C ring stretch. This peak shifted by ~30 $cm^{-1}$ to lower frequency with weak intensity. A similar weak peak at ~1340 $cm^{-1}$ is observed for the adsorption of catechol onto amorphous alumina surface and moderately strong peak for $Al^{3+}$–catechol complex [31]. Nevertheless, the multiple peaks in the range 1187–1281 $cm^{-1}$ correspond to phenolic –OH stretching and bending coupled with C–O stretching of free catechol, on adsorption, is located at 1256 $cm^{-1}$ as a single peak [39], for 3,4-DHBA it is at 1277 $cm^{-1}$. The strong peak at 1364 $cm^{-1}$ (C–C ring stretch coupled with C–O(H) bend) becomes weak upon adsorption and centered at 1331 $cm^{-1}$. For $Al^{3+}$–catechol complex these multiple peaks also disappear and a single and strong peak appears at 1260 $cm^{-1}$ [24]. Phenol, resorcinol and catechol adsorbed on metal oxide surfaces as phenoxide [31]. From the shifting of phenolic –OH bending and stretching

and the aromatic C–C stretch it is clear that catechol forms bidentate mononuclear surface complexes with α-alumina surfaces. The predicted surface complexation structure is shown in Fig. 6b.

## 4. Conclusions

At pH 5 catechol/α-alumina system takes less time (90 min) than the 3,4-DHBA/α-alumina (120 min) to reach the state of equilibrium that corresponds to lower activation energy for catechol than the 3,4-DHBA. But at pH 10 both the systems have nearly equal equilibration time (∼60 min). Further the adsorption kinetics of 3,4-DHBA and catechol at pH 10 and fixed initial concentration showed equivalent adsorption behaviour (Fig. 2). Thus, 3,4-DHBA exhibits equivalent adsorption pattern of catechol at pH 10 and we expect similar behaviour for 2,3-DHBA at higher alkaline pH and work are in progress. The UV spectral change of 3,4-DHBA at alkaline pH > 9 further demonstrate the deprotonation of phenolic –OH group. It indicates that at pH 10, 3,4-DHBA behaves like a catechol due to the deprotonation of –OH groups. Depending on the shifting of $\nu_{as}(-COO^-)$ and $\nu_s(-COO^-)$, it is concluded that 3,4-DHBA forms both outer- and inner-sphere surface complexes through $-COO^-$ and phenolic oxygen with α-alumina surfaces. Whereas for catechol the C–O(H) stretching and bending modes shifted and appeared as a single peak, reveal that catechol forms bidentate mononuclear surface complexes with α-alumina surfaces.

## Acknowledgements

The authors are grateful to the Department of Science and Technology and CSIR, New Delhi, India for the financial support and the Director, North-East Institute of Science and Technology, CSIR, Jorhat, India for the interest in this work and facilities. The authors are also thankful to Mr. P. Khound for recording the DRIFT spectra. We thank anonymous reviewers for a careful reading of the manuscript and constructive criticism thereafter.

## Appendix A. Supplementary data

Supplementary data associated with this article can be found, in the online version, at doi:10.1016/j.colsurfa.2011.07.024.

## References

[1] A. Chebbi, P. Carlier, Carboxylic acids in the troposphere, occurrence, sources, and sinks: a review, Atmos. Environ. 24 (1996) 4233–4249.
[2] B.W. Strobel, Influence of vegetation on low-molecular-weight carboxylic acids in soil solution—a review, Geoderma 99 (2001) 169–198.
[3] M. Kleber, R. Mikutta, M.S. Torn, R. Jahn, Poorly crystalline mineral phases protect organic matter in acid subsoil horizons, Eur. J. Soil Sci. 56 (2005) 717–725.
[4] K.-K. Au, A.C. Penisson, S. Yang, C.R. O'Melia, Natural organic matter at oxide/water interfaces: complexation and conformation, Geochim. Cosmochim. Acta 63 (1999) 2903–2917.
[5] R.G. Lehmann, H.H. Cheng, J.B. Harsh, Oxidation of phenolic acids by soil iron and manganese oxides, Soil Sci. Am. J. 51 (1987) 352–356.
[6] G.R. Aiken, in: P. MacCarthy (Ed.), Geochemistry, Isolation and Characterisation, John Wiley & Sons, New York, 1985, p. 363.
[7] U. Blum, Allelopathic interactions involving phenolic acids, J. Nematol. 28 (1996) 259–267.
[8] G.P. Sparling, D. Vaughan, Soil phenolic acids and microbes in relation to plant growth, J. Sci. Food Agric. 32 (1981) 625–626.
[9] R.H. Lima Leite, P. Cognet, A.M. Wilhelm, H. Delmas, Anodic oxidation of 2,4-dihydroxybenzoic acid for wastewater treatment, J. Appl. Electrochem. 33 (2003) 693–701.
[10] D.L. Norwood, J. Donald Johnson, R.F. Christman, J. Ronald Hass, M.J. Bobenrieth, Reactions of chlorine with selected aromatic models of aquatic humic material, Environ. Sci. Technol. 14 (1980) 187–190.
[11] K.V. Kumar, A. Shashi, A. Surendra, Adsorption of resorcinol and catechol on activated carbon: equilibrium and kinetics, Carbon 41 (2003) 765–773.
[12] F.M. Benoit, R. Helleur, M. Malaiyandi, S. Ramaswamy, D. Williams, Soil fulvic acid degradation by ozone in aqueous medium, Ozone: Sci. Eng. 15 (1993) 19–38.
[13] X.-H. Guan, C. Shang, G.-H. Chen, ATR-FTIR investigation of the role of phenolic groups in the interaction of some NOM model compounds with aluminum hydroxide, Chemosphere 65 (2006) 2074–2081.
[14] X.-H. Guan, G.-H. Chen, C. Shang, Combining kinetic investigation with surface spectroscopic examination to study the role of aromatic carboxyl groups in NOM adsorption by aluminum hydroxide, J. Colloid Interface Sci. 301 (2006) 419–427.
[15] M. Edward, M.M. Benjamin, J.N. Ryan, Role of organic acidity in sorption of natural organic matter (NOM) to oxide surfaces, Colloids Surf. A 107 (1996) 297–307.
[16] J.A. Davis, K.F. Hayes, Geochemical Processes at Mineral Surfaces, American Chemical Society, Washington, DC, 1986.
[17] R. Kummert, W. Stumm, The surface complexation of organic acids on hydrous γ-$Al_2O_3$, J. Colloid Interface Sci. 75 (1980) 373–385.
[18] C.R. Evanko, D.A. Dzombak, Influence of structural features on sorption of NOM-analogue organic acids to goethite, Environ. Sci. Technol. 32 (1998) 2846–2855.
[19] R. Backett, N.P. Le, The role of organic matter and ionic composition in determining the surface charge of suspended particles in natural waters, Colloids Surf. 44 (1990) 35–49.
[20] E. Tombacz, S. Barany, Role of Interfaces in Environmental Protection, Kluwer Academic Press, Amsterdam, 2003, p. 397.
[21] J.M. Borah, J. Sarma, S. Mahiuddin, Influence of functional groups on the adsorption behaviour of substituted benzoic acids at the α-alumina/water interface, Colloids Surf. A 375 (2011) 42–49.
[22] J.M. Borah, S. Mahiuddin, Adsorption and surface complexation of trimesic acid at the α-alumina–electrolyte interface, J. Colloid Interface Sci. 322 (2008) 6–12.
[23] Y. Chen, S. Liu, G. Wang, Kinetics and adsorption behavior of carboxymethyl starch on α-alumina in aqueous medium, J. Colloid Interface Sci. 303 (2006) 380–387.
[24] Y.S. Ho, Second-order kinetic model for the sorption of cadmium onto tree fern: a comparison of linear and non-linear methods, Water Res. 40 (2006) 119–125.
[25] Y.S. Ho, Review of second-order models for adsorption systems, J. Hazard. Mater. 136 (2006) 681–689.
[26] K.V. Kumar, Pseudo-second order models for the adsorption of safranin onto activated carbon: comparison of linear and non-linear regression methods, J. Hazard. Mater. 142 (2007) 564–567.
[27] S. Azizian, H. Bashiri, Adsorption kinetics at the solid/solution interface: statistical rate theory at initial times of adsorption and close to equilibrium, Langmuir 24 (2008) 11669–11676.
[28] E. Bulut, M. Özacar, İ.A. Şengil, Adsorption of malachite green onto bentonite: equilibrium and kinetics studies and process design, Micropor. Mesopor. Mater. 115 (2008) 234–246.
[29] T. Swain, Phenols and related compounds, in: R.M.C. Dawson, D.C. Elliott, W.H. Elliott, K.M. Jones (Eds.), Data for Biochemical Research, Oxford University Press, New York, 1969, p. 561.
[30] S.E. Blanco, M.C. Almandoz, F.H. Ferretti, Determination of the overlapping p$K_a$ values of resorcinol using UV–visible spectroscopy and DFT methods, Spectrochim. Acta Part A 61 (2005) 93–102.
[31] M.B. McBride, L.G. Wessellnk, Chemisorption of catechol on gibbsite, boehmite, and noncrystalline alumina surfaces, Environ. Sci. Technol. 22 (1988) 703–708.
[32] H. Gocmez, The interaction of organic dispersant with alumina: a molecular modelling approach, Ceram. Int. 32 (2006) 521–525.
[33] L. Ohrstrom, I. Michand-Soret, Fe-catecholate and Fe-oxalate vibrations and isotopic substitution shift from DFT quantum chemistry, J. Phys. Chem. A 103 (1999) 256–264.
[34] T. Lana-Villarreal, A. Rodes, J.M. Perez, R. Gomex, A spectroscopic and electrochemical approach to the study of the interactions and photoinduced electron transfer between catechol and anatase nanoparticles in aqueous medium, J. Am. Chem. Soc. 36 (2005) 12601–12611.
[35] G. Scorates, Infrared & Raman Group Frequency Tables and Charts, John Wiley & Sons, New York, 2001.
[36] G. Varsanyl, S. Szoke, Vibrational Spectra of Benzene Derivatives, Academic Press, New York, 1969.
[37] K.H. Kung, M.B. McBride, Coordination complexes of *p*-hydroxybenzoate on Fe oxides, Clays Clay Miner. 37 (1989) 333–340.
[38] M. Biber, W. Stumm, An in-situ ATR-FTIR study: the surface coordination of salicylic acid on aluminum and iron(III) oxides, Environ. Sci. Technol. 28 (1994) 763–768.
[39] H. Gulley-Stall, P.A. Hogam II, W.L. Schmidt, S.J. Wall, A. Buhrlage, H.A. Bullen, Surface complexation of catechol to metal oxides: an ATR-FTIR adsorption and dissolution study, Environ. Sci. Technol. 44 (2010) 4116–4121.
[40] P.Z. Araujo, C.B. Mendive, L.A.G. Rodenas, P.J. Morando, A.E. Regazzoni, M.A. Blesa, D. Bahnemann, FT-IR-ATR as a tool to probe photocatalytic interfaces, Colloids Surf. A 265 (2005) 73–80.
[41] P.Z. Araujo, P.J. Modando, M.A. Blesa, Interaction of catechol and gallic acid with titanium dioxide in aqueous suspensions. I. Equilibrium studies, Langmuir 21 (2005) 3470–3474.
[42] J. Arana, E.P. Melian, V.M.R. Lopez, A.P. Alonso, J.M.D. Rodriguez, O.G. Diaz, J.P. Pena, Photocatalytic degradation of phenol and phenolic compounds: Part I. Adsorption and FTIR study, J. Hazard. Mater. 146 (2007) 520–528.
[43] E.C. Yost, M.I. Tejedor-Tejedor, M.A. Anderson, In situ CIR-FTIR characterization of salicylate complexes at the goethite/aqueous solution interface, Environ. Sci. Technol. 24 (1990) 822–828.